Obtaining the Kinetic Function of Depolymerization from Evolving Molecular Weight Distribution Data–An Inverse Problem

Y. Leong Yeow, Bifei Guan, Liang Wu, and Tze-Ming Yap
Dept. of Chemical and Biomolecular Engineering, The University of Melbourne, Victoria 3010, Australia

Jong-Leng Liow
School of Engineering and Information Technology, The University of New South Wales at ADFA, Canberra ACT 2600, Australia

Yee-Kwong Leong
School of Mechanical and Chemical Engineering, University of Western Australia, Crawley 6009, Australia

DOI 10.1002/aic.13878
Published online July 3, 2012 in Wiley Online Library (wileyonlinelibrary.com).

Depolymerization of macromolecules is generally regarded as a first order process with a kinetic function that depends on the molecular weights of the fragmenting molecule and fragmentation products. This article describes a computation scheme for obtaining the kinetic function from observed molecular weight distribution (MWD) data. The integro-differential equation used by most investigators to compute MWD with some assumed kinetic function is reformulated as an inverse problem in which the kinetic function is treated as the unknown to be extracted from evolving MWD data. A numerical procedure based on two consecutive applications of Tikhonov regularization is developed to solve this inverse problem. It gives the kinetic function as the solution of a set of linear algebraic equations. Implementation of this procedure is described in full and its performance is assessed by applying it to simulated MWD data. A number of issues associated with discretization and regularization are discussed. © 2012 American Institute of Chemical Engineers *AIChE J,* 59: 912–922, 2013
Keywords: computational chemistry (kinetics/thermo), polymerization, reaction kinetics, flocculation

Introduction

Depolymerization kinetics of macromolecules is not only of interest to polymer chemists but also to chemical engineers as it is central to the understanding of processes such as cracking of heavy petroleum fractions and depolymerization of waste plastics for possible recycling as industrial raw materials. In the laboratory macromolecules are cleaved, for example, by sonication, by chemical or biochemical reactions and thermally into a large collection of small fragments of different sizes. As depolymerization progresses the ratio between the maximum m_{max}, and minimum m_{min} molecular weight of the fragments observed can be 10^3 or larger. Consequently, it is no longer a fruitful exercise to track the increase or reduction in concentration of each individual macromolecular species.[1] Instead, the molecular weight m is treated as a continuous variable and the progress of the depolymerization process is quantified by a concentration density function $c(t, m)$ that depends on two continuous variables; depolymerization time t and molecular weight m. At any time t the molar concentration of the fragment with molecular weight between $m\text{-}\delta m/2 \leq m \leq m+\delta m/2$ is given by $c(t, m)\delta m$. The total mass, m_{total}, of the macromolecules which remains constant during the depolymerization process is given by the first moment of the concentration density function. Results of depolymerization investigation are routinely presented as plots of $c(t, m)$ vs. m with t treated as an independent parameter held fixed on each plot. They are referred to as molecular weight distribution (MWD) curves and provide a very vivid picture of the progress of the depolymerization process. Until recently the determination of MWD in the laboratory was not simple to perform and MWD curves were reported only for a very small numbers of discrete time steps—often just the initial MWD and that at the end of the experiment. With the advances in instrumental analysis techniques, particularly in gel permeation chromatography (GPC), more MWD curves, as many as 5 to 10 measurement time steps, spreading over a depolymerization time of 10 to 20 hours are now appearing in the literature.[2–5] Future automation of GPC is likely to increase the number of measurement time steps opening up new approaches in quantitative investigation of the kinetics of depolymerization.

Mass balance of size m macromolecules, for $m_{min} < m < m_{max}$, during the depolymerization process leads directly to an integro-differential equation for $c(t, m)$. This equation is closely related to the population balance equation (PBE) (Eq. 1) widely used in the investigation of flocculation

Correspondence concerning this article should be addressed to Y. L. Yeow at yly@unimelb.edu.au.

processes.[6,7] This equation coupled with the initial MWD curve $c(0, m)$ can be solved by a variety of techniques to yield the computed MWD curves for a preassumed depolymerization kinetics. This route to computed MWD curves is generally referred to as the direct problem of depolymerization. One of these techniques for the direct problem is the method of lines (MoL).[8,9] Comparison of the computed MWD curves against the corresponding experimental curves is then used to test the validity and to improve the assumed depolymerization kinetics. The general approach here is to adjust the numerical parameters in the preassumed kinetics so that the computed MWD curves match up with their experimental counterpart. Such an approach has a number of obvious drawbacks. Chief among these is that it requires, at the very outset of the MWD computation, the adoption of a specific functional form of the depolymerization kinetics from a bewildering array of possible forms. Very frequently this approach does not lead to a well-defined kinetics for a given set of MWD curves.

The present investigation adopts an entirely different approach to the determination of the kinetics of macromolecule depolymerization. Its aim is to extract the depolymerization kinetics directly from a set of general evolving MWD curves without having to solve the PBE as an integro-differential equation and without making specific assumption regarding the functional form of the kinetic function. Mathematically this problem is known as the inverse problem of depolymerization. The treatment of this inverse problem in the present investigation differs significantly from that adopted by, for example, Sathyagal et al.[10] in which they assumed that the kinetic functions for self-similar MWD curves can be represented by a preselected set of basis functions. A consequence of the more general treatment adopted here means that the inverse problem is ill-posed and specialized solution techniques are required. In this investigation, Tikhonov regularization will be used.[11,12] This is a specialized technique for handling a wide range of inverse problems. The formulation of the inverse problem and the associated numerical solution steps will be described. To ensure ease of adoption of the solution technique by would be users the key formulation steps are described in detail. A general purpose commercial scientific computing software is used to perform all the numerical steps so that no specialized software is required. The efficacy of the procedure is demonstrated through a number of examples to show its reliability and general applicability.

Kinetic Function and the Inverse Problem of Depolymerization

The governing equation for $c(t, m)$ is

$$\frac{\partial c(t,m)}{\partial t} = \int_{m_r=m+m_{\min}}^{m_{\max}} k(m_r,m)c(t,m_r)dm_r - \frac{c(t,m)}{2}\int_{m_p=m_{\min}}^{m-m_{\min}} k(m,m_p)dm_p \quad (1)$$

This is an abridged form of the PBE.[13] For brevity the subscript used to indicate that m is held fixed in the temporal derivative on the LHS has been suppressed. It is tacitly assumed that depolymerization conditions are such that molecules do not combine to form larger ones and consequently the terms associated with aggregation in the full PBE have been left out in Eq. 1. The first integral on the RHS gives the rate of formation of size m macromolecule arising from the disintegration of larger macromolecules m_r into m and $m_r - m$ (where $m_r > m$). The second integral gives the rate of disappearance of macromolecule m as a result of its disintegration into smaller fragments m_p and $m - m_p$ (where $m_p < m$). The numerical coefficient 1/2 is to correct for the double counting associated with this integral. The difference between the two integrals gives the accumulation or depletion rate of size m molecules, *i.e.*, $\partial c(t, m)/\partial t$.

Implicit in Eq. 1 is the simple assumption that the rate of binary fragmentation of size m_r macromolecule

$$m_r \rightarrow m_p + (m_r - m_p) \quad (2)$$

is proportional to $c(m_r, t)$. The complication here is that the "constant" of proportionality changes with the molecular weight m_r and also with that of the products m_p, $m_r - m_p$.[1]

$$\text{Fragmentation rate} = -k(m_r, m_p)c(m_r, t) \quad (3)$$

This dependence is made explicit by using $k(m_r, m_p)$, the kinetic function, to denote the "constant." The way the kinetic function varies with m_r and m_p characterizes the binary fragmentation behavior of the macromolecule. Apart from the requirement that $k(m_r, m_p)$ be a well-behaved positive function with $k(m_r, m_p) = k(m_r, m_r - m_p)$ its functional form is generally not known and has to be determined either from observed MWD data or from depolymerization mechanism considerations.

Even though both the direct problem and the inverse problem of depolymerization are based on Eq. 1 the mathematical nature of the two problems are entirely different and require completely different solution procedure. In the direct problem Eq. 1 is an integro-differential equation for the unknown $c(t, m)$. This is a well-posed problem with well-established methods of solution.[14] In the inverse problem, Eq. 1 becomes an integral equation of the first kind for the unknown kinetic function $k(m_r, m_p)$. Such an integral equation is known to be an ill-posed problem in which noise amplification is a serious issue.[11] There are no generally accepted methods of solution. In this investigation, through a series of preprocessing steps the integral equation is converted into a set of linear algebraic equations to be solved, together with Tikhonov regularization to suppress noise, for the unknown $k(m_r, m_p)$.

The first preprocessing step is to compute the temporal derivative $\partial c(t, m)/\partial t$ on the LHS of Eq. 1 from the observed MWD data. This step in itself is an inverse problem and will be referred to as the first inverse problem to distinguish it from the main inverse problem of solving for the kinetic function $k(m_r, m_p)$. The latter will be referred to as the second inverse problem. As the name implies the first inverse problem also suffers from unavoidable noise amplification.[11] In the present investigation, the temporal derivatives of the first inverse problem will be obtained using the numerical procedure described by Lubansky et al.[15] Their procedure also relies on Tikhonov regularization to keep noise amplification under control. The $\partial c(t, m)/\partial t$ is computed for a set of selected molecular weights $\mathbf{m}_{selm} = [m_{selm1}, m_{selm2}, \ldots m_{selm\sigma}, \ldots, m_{selm\Sigma}]^T$. It is a small subset, typically consisting of $\Sigma = 9$ to 15 points, of the large set of uniformly spaced discretization grid points (to be introduced below) of

the independent variable $m_{\min} \le m \le m_{\max}$. Provided the available MWD curves include a large enough number of measurement time steps, typically larger than about 15, experience shows that Tikhonov regularization is able to cope with the usual random measurement noise in $c(t, m)$ to yield the temporal derivatives reliably.

With the numerically obtained derivatives $\partial c(t, m_{\text{selm}})/\partial t$ and the MWD data regarded as known input, it is more fitting to rewrite Eq. 1 as

$$\int_{m_r=m_{\text{selm}}+m_{\min}}^{m_{\max}} k(m_r, m_{\text{selm}})c(t, m_r)dm_r - \frac{c(t, m_{\text{selm}})}{2} \int_{m_p=m_{\min}}^{m_{\text{selm}}-m_{\min}} k(m_{\text{selm}}, m_p)dm_p = \frac{\partial c(t, m_{\text{selm}})}{\partial t} \quad (4)$$

This is the integral equation of the first kind mentioned above that will be converted into a set of linear algebraic equation for the unknown kinetic function $k(m_r, m_p)$. It is the starting point of the second inverse problem. This integral equation has multiple known RHS - one arising from each member of the set of selected molecular weights $\mathbf{m}_{\text{selm}}$. The independent variables are t and m_{selm} and the kernel of the integral equation is $c(t, m_r)$ in the first integral and unity in the second integral.

To ensure generality all the computation steps for the kinetic function will be based on a dimensionless equivalent of Eq. 4. To this end the following dimensionless variables are introduced

$$\begin{aligned} &M \equiv m/m_{\max}, \quad M_r = m_r/m_{\max}, \quad M_p = m_p/m_{\max}, \\ &M_{\text{selm}} \equiv m_{\text{selm}}/m_{\max}, \\ &\tau \equiv t/t_{\max}, \quad t_{\text{selt}} \equiv t_{\text{selt}}/t_{\max}, \\ &C(\tau, M) \equiv (m_{\max})^2 c(t, m)/m_{\text{total}}, \\ &K(M_r, M_p) \equiv (t_{\max} \times m_{\max})k(m_r, m_p). \end{aligned} \quad (5)$$

These led directly to the dimensionless equivalent of Eq. 4

$$\int_{M_r=M_{\text{selm}}+M_{\min}}^{1} K(M_r, M_{\text{selm}})C(\tau, M_r)dM_r - \frac{C(\tau, M_{\text{selm}})}{2} \times \int_{M_p=M_{\min}}^{M_{\text{selm}}-M_{\min}} K(M_{\text{selm}}, M_p)dM_p = \frac{\partial C(\tau, M_{\text{selm}})}{\partial \tau} \equiv H(\tau, M_{\text{selm}}). \quad (6)$$

In this dimensionless equation of the second inverse problem the dimensionless time varies between $0 \le \tau \le 1$ and the dimensionless molecular weight between $M_{\min} \le M_r, M_p \le 1$. As $m_{\min} << m_{\max}$ in most depolymerization investigation, its dimensionless counterpart will be approximated by $M_{\min} = 0$ in all the examples below. The definition of $C(\tau, M)$ means that its first moment is equal to unity for all τ.

To make discretization of Eq. 6 and the associated matrix manipulations easier to follow the numerically evaluated derivative $\partial C(\tau, M_{\text{selm}})/\partial \tau$ will be denoted by $H(\tau, M_{\text{selm}})$ and treated as a known function of τ and M_{selm}.

Discretized independent variables, kinetic function, and integral equation

In the numerical scheme to solve the second inverse problem the discretized molecular weight $0 \le M \le 1$ will be denoted by the column vector $\mathbf{M} = [M_1 = 0, M_2, \ldots M_j, \ldots M_{N_D} = 1]^T$. Typically the number of discretization points in $\mathbf{M}$ is $N_D = 51$ or 101 or 201. In the solution scheme, the discretized equivalent of Eq. 6 will be met at a set of selected dimensionless time τ denoted by the column vector $\boldsymbol{\tau}_{\text{selt}} = [\tau_{\text{selt1}}, \tau_{\text{selt2}}, \ldots, \tau_{\text{selt}\psi}, \ldots \tau_{\text{selt}\Psi\text{-}1}, \tau_{\text{selt}\Psi}]^T$. This is a subset of the measurement time steps at which the MWD curves $C(\tau, M)$ are available. The size of $\boldsymbol{\tau}_{\text{selt}}$ is relatively small; typically $5 \le \Psi \le 10$. As mentioned earlier, $\mathbf{M}_{\text{selm}}$, the selected molecular weight at which $H(\tau, M_{\text{selm}}) \equiv \partial C(\tau, M_{\text{selm}})/\partial \tau$ are evaluated, is a subset of $\mathbf{M}$. For example, for $N_D = 101$, a typical subset is $\mathbf{M}_{\text{selm}} = [M_{11}, M_{21}, M_{31}, \ldots, M_{91}]^T$, i.e., every tenth internal points of the discretization grid.

The unknown function $K(M_r, M_p)$ after discretization takes the form of a two-dimensional (2-D) matrix $\mathbf{K}$ with elements $K_{i,j}$ where $1 \le i, j \le N_D$. The first index is associated with the fragmenting macromolecule M_r and second index is with that of the product of fragmentation M_p. Even for a relatively moderate N_D of 51 or 101 or 201 $\mathbf{K}$ is a very large matrix. However, because of the physical properties of the kinetic function, the number of independent unknown $K_{i,j}$ to be determined is much smaller. For example, as $0 \le M_p \le M_r$ this leads directly to the restriction $j < i$ thereby cutting the number of physically relevant and unknown $K_{i,j}$ by half. The physical requirement $K(M_r, M_p) = K(M_r, M_r - M_p)$ reduces the number of independent $K_{i,j}$ by a further factor of 2. As macromolecules with $M_p = M_{\min}$ are not observed consequently $K(M_r, 0) = K(M_r, M_r) = 0$ for any $0 \le M_r \le 1$. These are eliminated from the list of unknown $K_{i,j}$. All the reductions in the number of unknown $K_{i,j}$ are summarized by

$$\begin{aligned} K_{i,1} = &K_{i,i} = 0 \text{ for any } i \\ &K_{i,j} \text{ is defined only for } j < i \\ &K_{i,j} = K_{i,i-j} \end{aligned} \quad (7)$$

In the solution scheme for the kinetic function instead of treating the independent unknown $K_{i,j}$ as elements of a 2-D matrix they are grouped together and treated as the elements of an unknown column vector $\boldsymbol{\Gamma} = [\Gamma_1, \Gamma_2, \ldots \Gamma_\lambda, \ldots \Gamma_\Lambda]^T$. A simple two-way mapping can be defined between the elements of Γ_λ and $K_{i,j}$. For example, as the first nontrivial unknown element of $\mathbf{K}$ is $K_{3,2}$ thus $\Gamma_1 = K_{3,2}$. It follows that $\Gamma_2 = K_{4,2} = K_{4,3}$, $\Gamma_3 = K_{5,2} = K_{5,4}$, $\Gamma_4 = K_{5,3}$, etc. Λ, the total number of unknown Γ_λ, depends on N_D. For example, for $N_D = 101$ the total number of elements in $\mathbf{K}$ is $101 \times 101 = 10{,}201$ but the size of the corresponding $\boldsymbol{\Gamma}$ is only $\Lambda = 2{,}500$.

To satisfy Eq. 6 at the set of selected time $\boldsymbol{\tau}_{\text{selt}}$ for the set of selected molecular weight $\mathbf{M}_{\text{selm}}$, the known numerical values of $H(\tau, M_{\text{selm}})$ on the RHS, after discretization, will also result in a 2-D matrix $\mathbf{H}$ with typical element $H_{\text{selt, selm}}$ where the two indices correspond to the indices of $\boldsymbol{\tau}_{\text{selt}}$ and $\mathbf{M}_{\text{selm}}$, respectively. As with $\mathbf{K}$, the elements of the matrix $\mathbf{H} = [\{H_{\text{selt1,selm1}}, H_{\text{selt1,selm2}}, \ldots H_{\text{selt1,selm}\Sigma}\}, \{H_{\text{selt2,selm1}}, H_{\text{selt2,selm2}}, \ldots H_{\text{selt2,selm}\Sigma}\}, \ldots \{H_{\text{selt}\Psi,\text{selm1}}, H_{\text{selt}\Psi,\text{selm2}}, \ldots H_{\text{selt}\Psi,\text{selm}\Sigma}\}]$ will also be treated as a column vector in the solution process. This known column vector will be denoted by $\boldsymbol{\Phi} = [\Phi_1, \Phi_2, \ldots \Phi_\omega, \ldots \Phi_\Omega]^T$. The elements of $\boldsymbol{\Phi}$ are related to that of $\mathbf{H}$, for example, $\Phi_1 = H_{\text{selt1,selm1}}$, $\Phi_2 = H_{\text{selt1,selm2}}$, etc. The size of the column vector $\boldsymbol{\Phi}$ is therefore given by $\Omega = \Psi \times \Sigma$. - the number of Eq. 6 that has to be satisfied. Typically this is around 40 to 80.

In terms of the discretized variables, the discretized equivalent of Eq. 6 is

$$\sum_{i=\text{selm}+1}^{N_D} \mu_{i,\text{selm}} K_{i,\text{selm}} C_{\text{selt},i} \Delta - \frac{C_{\text{selt,selm}}}{2} \sum_{j=2}^{\text{selm}-1} v_{\text{selm},j} K_{\text{selm},j} \Delta = H_{\text{selt,selm}} \quad 1 \le \text{selt} = \Psi, \quad 1 \le \text{selm} \le \Sigma \tag{8}$$

The two integrals in the original equation, approximated by quadrature using the trapezoidal rule, now appear as two summations. $\mu_{i,\text{selm}}$ and $v_{\text{selm},j}$ are numerical coefficients associated with the trapezoidal rule, i.e., $\mu_{i,\text{selm}}$ and $v_{\text{selm},j} = 1$ for discretization points in the interior of the integrals and 1/2 at the end points of the integrals. $\Delta = (1 - M_{\min})/(N_D - 1)$ is the discretization step size. For any combination of the indices i, selt and selm the coefficients $C_{\text{selt},i}$ and $C_{\text{selt,selm}}$ are known numerical quantities given by the MWD curves.

Thus the LHS of Eq. 8 can be treated as a linear combination of the unknown elements of $\mathbf{K}$, i.e., of $\mathbf{\Gamma} = [\Gamma_1, \Gamma_2, \ldots \Gamma_\lambda, \ldots \Gamma_\Lambda]^T$ and the RHS is an element of the known column vector derived from $\mathbf{H}$, i.e., of $\mathbf{\Phi} = [\Phi_1, \Phi_2, \ldots \Phi_\omega, \ldots \Phi_\Omega]^T$. This is the linear algebraic equations of the second inverse problem which can be written in a compact matrix form

$$\mathbf{G\Gamma} = \mathbf{\Phi} \tag{9}$$

where $\mathbf{G}$ is a $\Omega \times \Lambda$ matrix. The row order of $\mathbf{G}$ is the same as the order by which the elements of $\mathbf{H}$ are arranged in $\mathbf{\Phi}$. Within a row of $\mathbf{G}$ the numerical value of its elements are given by $\mu_{i,\text{selm}} C_{\text{selt},i} \Delta$ or $-C_{\text{self,selm}} v_{\text{selm},j} \Delta/2$. The location of these coefficients within the row is determined by the running indices i and j according to the two-way mapping between Γ_λ and $K_{i,j}$. Elements not covered by the two running indices are identically zero. In short all the elements of $\mathbf{G}$ are known numerical coefficients.

$\mathbf{G}$ is not a square matrix and therefore does not have an inverse. An approximate solution $\mathbf{\Gamma}$ to Eq. 9 can be obtained by minimizing the sum of squares (SoQ) of the deviation of $\mathbf{G\Gamma}$ from the known computed temporal derivatives $\mathbf{\Phi}$, i.e., minimizing

$$\text{SoQ[deviation]} = [G\mathbf{\Gamma} - \mathbf{\Phi}]^T [\mathbf{G\Gamma} - \mathbf{\Phi}] \tag{10}$$

However, such a solution is likely to exhibit unphysical fluctuations making it unacceptable. Tikhonov regularization is applied to keep the fluctuations under control.[11]

Kinetic function based on Tikhonov regularization

In the present investigation the fluctuation exhibited by $\mathbf{\Gamma}$ is suppressed by requiring its elements Γ_λ to minimize the sum of squares of $\partial^2 K/\partial M_r^2$ and that of $\partial^2 K/\partial M_p^2$ at internal discretization points. This condition is to be imposed simultaneously with the minimization of the SoQ in Eq. 10. For this purpose the second partial derivatives of $K_{i,j}$ at a typical discretization point are approximated by central finite difference

$$\frac{\partial^2 K_{i,j}}{\partial M_r^2} = \frac{K_{i+1,j} + K_{i-1,j} - 2K_{i,j}}{\Delta^2} \quad \text{for } 3 \le i \le N-1, \quad 1 < j \le i-1 \tag{11a}$$

$$\frac{\partial^2 K_{i,j}}{\partial M_p^2} = \frac{K_{i,j+1} + K_{i,j-1} - 2K_{i,j}}{\Delta^2} \quad \text{for } 3 \le i \le N, \quad 1 < j \le i-1 \tag{11b}$$

The limits placed on the indices in these expressions are such that no unknown $K_{i,j}$ outside the range covered by the MWD data will be introduced. After the elements of $\mathbf{K}$ in these expressions are replaced by their equivalents in the column vector $\mathbf{\Gamma}$, Eq. 11 can be put in the form of linear combinations of the elements of this vector

$$\frac{\partial^2 \Gamma_\zeta}{\partial M_r^2} = E_\zeta = \sum_{\lambda=1}^{\Lambda} \alpha_{\zeta,\lambda} \Gamma_\lambda \quad \text{or} \quad \mathbf{E} = \boldsymbol{\alpha}\mathbf{\Gamma} \tag{12a}$$

$$\frac{\partial^2 \Gamma_\zeta}{\partial M_p^2} = F_\zeta = \sum_{\lambda=1}^{\Lambda} \beta_{\zeta,\lambda} \Gamma_\lambda \quad \text{or} \quad \mathbf{F} = \boldsymbol{\beta}\mathbf{\Gamma} \tag{12b}$$

where $\boldsymbol{\alpha}_{\zeta,\lambda}$ and $\boldsymbol{\beta}_{\zeta,\lambda}$ are known numerical coefficients arising from standard central difference approximation of second derivative. $\boldsymbol{\alpha}$ and $\boldsymbol{\beta}$ are sparse matrices. For a given Γ_ζ, only those coefficients associated with the immediate neighbors of $K_{i,j}$ that corresponds to Γ_ζ are nonzero while all other elements are identically zero. Column vectors $\mathbf{E}$ and $\mathbf{F}$ are shorthand notations used to represent the second derivatives to simplify the subsequent matrix manipulations. Equation 12 can be further simplified by combining the column vectors $\mathbf{E}$ and $\mathbf{F}$ and the matrices of coefficients $\boldsymbol{\alpha}$ and $\boldsymbol{\beta}$ leading to a single matrix equation for both of the second derivatives

$$\mathbf{D} = \begin{pmatrix} \mathbf{E} \\ \mathbf{F} \end{pmatrix} = \begin{pmatrix} \boldsymbol{\alpha} \\ \boldsymbol{\beta} \end{pmatrix} \Gamma = \mathbf{A\Gamma} \tag{13}$$

$\mathbf{D}$ is the combined column vector of the second derivatives to be kept small and $\mathbf{A}$ is a known composite sparse matrix of numerical coefficients consisting mainly of 0's with $1/\Delta^2$ or $-2/\Delta^2$ at the appropriate locations. To suppress excessive fluctuation in $\mathbf{\Gamma}$ the SoQ of the elements of $\mathbf{D}$ is minimized. In terms of Eq. 13 this reduces to minimizing

$$SoQ(\mathbf{D}) = (\mathbf{A\Gamma})^T \mathbf{A\Gamma} = \mathbf{\Gamma}^T \mathbf{A}^T \mathbf{A\Gamma} \tag{14}$$

The matrix $\mathbf{A}$ which depends only on N_D and the two-way mapping between $\mathbf{K}$ and $\mathbf{\Gamma}$ will be referred to as the smoothness matrix.

In Tikhonov regularization instead of meeting the accuracy condition represented by Eq. 10 or the smoothness condition represented by Eq. 14 separately the following sum of the two SoQs is minimized.

$$R = [\mathbf{G\Gamma} - \mathbf{\Phi}]^T [\mathbf{G\Gamma} - \mathbf{\Phi}] + \chi \mathbf{\Gamma}^T \mathbf{A}^T \mathbf{A\Gamma} \tag{15}$$

R is referred to as the residual and χ, a positive constant, is the Tikhonov regularization parameter. A large χ favors a smooth solution and a small χ ensures that Eq. 9 is closely satisfied. The $\mathbf{\Gamma}$ that minimizes R is given by[12,16]

$$\mathbf{\Gamma} = [\mathbf{G}^T \mathbf{G} + \chi \mathbf{A}^T \mathbf{A}]^{-1} \mathbf{G}^T \mathbf{\Phi} \tag{16}$$

The regularization parameter χ is not a kinetic property of the depolymerization system under investigation. It depends on the noise level in the MWD data and on the number of discretization points. In all the examples in the next section χ will be selected so that the resulting average deviation in Eq. 9

is comparable with the estimated error bar in the computed temporal derivatives $\mathbf{\Phi}$. This is often referred to as the Morozov principle in the inverse problem literature.[11] In addition, the choice of χ will also be guided by the expectation that the resulting kinetic function $K(M_r, M_p)$ should be physically meaningful.

Results

The performance of the solution scheme described above will now be tested by using Eq. 16 to extract the kinetic function $K(M_r, M_p)$, via $\mathbf{\Gamma}$, from a number of sets of evolving MWD curves $C(\tau, M)$. These curves are the solutions of the direct problem of depolymerization generated by MoL. Working with simulated $C(\tau, M)$ allows the $K(M_r, M_p)$ given by Eq. 16 to be checked against that used in the direct problem. At the same time it will reveal the practical requirements placed on MWD curves $C(\tau, M)$ by the inverse problem and the critical steps in the solution procedure. All the independent variables, MWD curves and kinetic functions in the following examples are in the dimensionless form introduced above.

Simple simulated MWD curves

This example is based on the simulated MWD curves generated by MoL with the kinetic function

$$K(M_r, M_p) = 60M_p(M_r - M_p), M_p \leq M_r. \qquad (17)$$

This is shown graphically in Figure 1a where M_r is kept constant on each curve while M_p varies between $0 \leq M_p \leq M_r$. This kinetics is based on the simple but physically realistic assumption that in binary fragmentation larger molecules generally disintegrate at a higher rate than smaller ones. It further assumes that when a macromolecule disintegrates it is more likely to break into two fragments of similar size than two that are vastly different in size.[17] The numerical factor on the RHS of Eq. 17 is the constant of proportionality between fragmentation rate and M_p and $(M_r - M_p)$ and its numerical value depends on the time scale of the problem.

A set of simulated MWD curves based on Eq. 17 is shown in Figure 1b. These are plots of $C(\tau, M_r)$ against M_r with τ, treated as a parameter, kept constant for each curve. These curves for the 17 measurement time steps shown in the figure, simulate experimental measurements that monitor the temporal progress of depolymerization. The broken curve is the arbitrary initial condition. Mass preservation of macromolecules (better than 99%) was performed to check the reliability of these simulated results.

To generate the temporal derivative $H(\tau, M) \equiv \partial C(\tau, M)/\partial\tau$ on the RHS of Eq. 6, the curves in Figure 1b, for selected molecular weight $\mathbf{M}_{selm}$, are replotted as function of τ in Figures 2a, b. The 11 members of $\mathbf{M}_{selm}$ are shown in the figure caption. When differentiated numerically with respect to τ the resulting $\partial C(\tau, M)/\partial\tau$ curves are shown in Figure 2c. With 17 measurement time steps on each of the curves in Figures 2a, b the numerical differentiation procedure of Lubansky et al. was able to generate the temporal derivatives reliably—particularly at the interior of $0 < \tau < 1$.[15] To keep the changes to the computer code for the first inverse problem to a minimum the number of discretization points in the interval $0 \leq \tau \leq 1$ was kept fixed at 101 in this example and also in the following two examples.

The discrete points in Figure 2c are the temporal derivatives at six selected dimensionless time $\boldsymbol{\tau}_{selt}$ = [0.3, 0.35, 0.4, 0.5, 0.6, 0.7]^T. These are stored as the column vector $\mathbf{\Phi}$ on the RHS of Eq. 9. $\boldsymbol{\tau}_{selt}$, as can be observed from Figure 2c, is an internal subset of the 17 measurement time steps in Figure 1b. There are $6 \times 11 = 66$ elements in $\mathbf{\Phi}$.

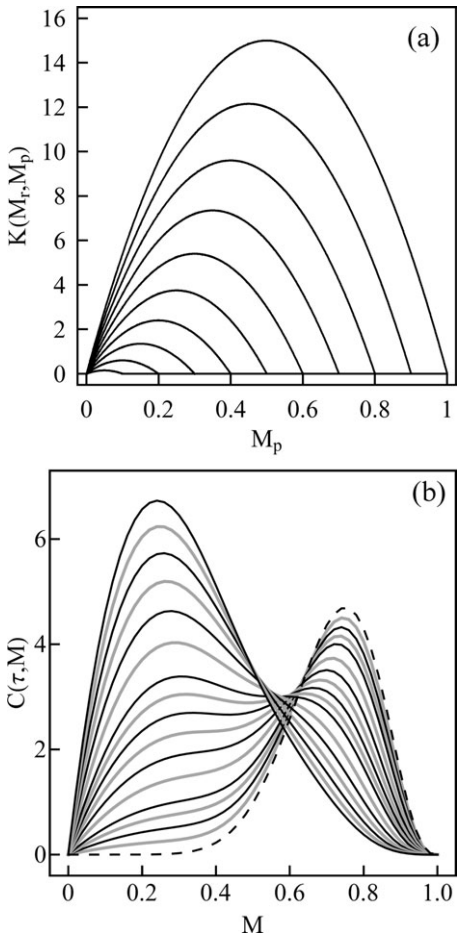

Figure 1. Simple kinetic function and MWD curves.

(a) Variation of kinetic function $K(M_r, M_p)$ from Eq. 17 with M_p. M_r is kept fixed on each curve. $M_r = 0.1$ (left most), 0.2, …0.9, 1.0 (right most). (b) Simulated MWD curves $C(\tau, M)$ based the kinetics in (a) for measurement time steps $\tau = 0$ (broken curve), 0.025, 0.05, 0.075, 0.1, 0.15, 0.2, 0.25, 0.3, 0.35, 0.4, 0.5, 0.6, 0.7, 0.8, 0.9, 1(left most).

Substitution of the $\mathbf{\Phi}$ and $\mathbf{G}$ derived from the simulated MWD curves in Figure 1b together with the smoothness matrix $\mathbf{A}$ of the discretization scheme into Eq. 16 yields $\mathbf{\Gamma}$ and hence the discretized $K(M_r, M_p)$ directly. These are shown as discrete points in Figure 3. For comparison the curves from Figure 1a are shown as lighter curves on the same plot. It is clear that, apart from the small deviation for $M_r = 1$, the kinetic function given by Eq. 16 is in very good agreement with that assumed in the direct problem.

As a further check the depolymerization kinetics as represented by the discrete points in Figure 3 is used in the solution, by MoL, of the direct problem of depolymerization. To this end these discrete points are interpolated locally, with cubic polynomials, to generate a continuous kinetic function $K(M_r, M_p)$ needed in the MoL computation. The resulting MWD curves of the direct problem are essentially indistinguishable from that in Figure 1b confirming the reliability of the solution to the inverse problem given by Eq. 16. Interpolation of the computed discrete kinetic data was carried out automatically by standard scientific computing software

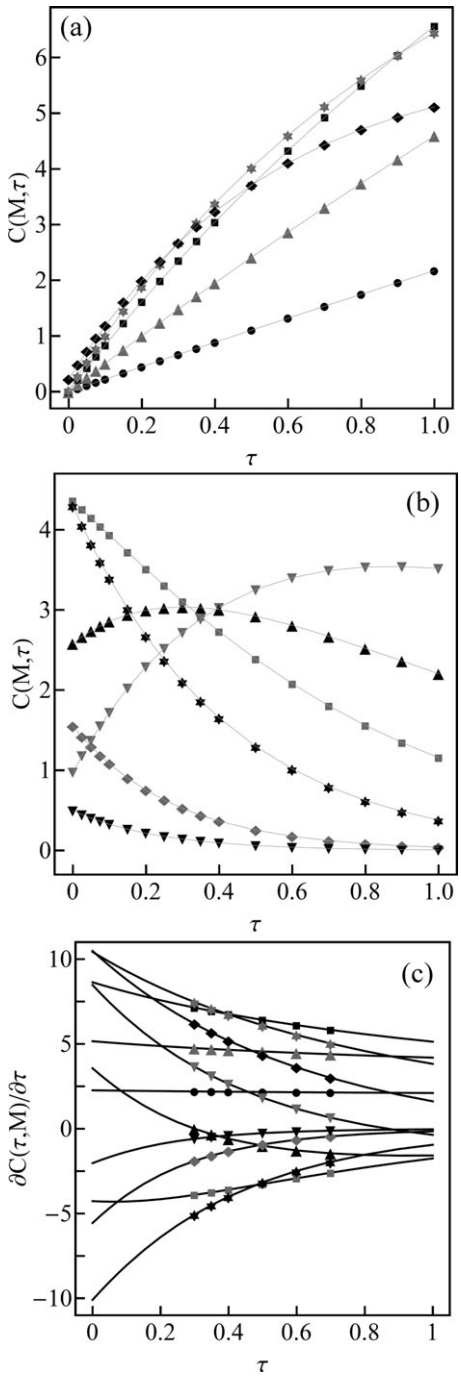

Figure 2. Temporal variation and temporal derivatives of $C(\tau, M)$.

(a) and (b) Plots of $C(\tau, M)$ based on Eq. 17 against τ. On each curve M is kept fixed at the indicated molecular weight $\mathbf{M}_{selm}$ = [0.04(●), 0.1(▲), 0.2(■), 0.3(★), 0.4(◆), 0.5(▼), 0.6(▲), 0.7(■), 0.8(★), 0.9(◆), 0.94(▼)]^T. (c) Variation of temporal derivatives with τ for the $\mathbf{M}_{selm}$ in (a) and (b). Discrete points are the derivatives at τ_{selt} = [0.3, 0.35, 0.4, 0.5, 0.6, 0.7]^T.

requiring no additional input. Besides MoL computation, the interpolated function can be used in any computation involving $K(M_r, M_p)$. The only restriction is that it should not be differentiated as this will amplify the unavoidable noise present in the discrete points in Figure 3.

In this example, $N_D = 51$ for the discretization of $0 \leq M \leq 1$. Refinement of the discretization did not result in observable difference in the resulting kinetic function. For the results in Figure 3, the Tikhonov regularization parameter $\chi = 0.001$. As frequently observed in Tikhonov regularization computations, these results are not very sensitive to changes in χ. Halving or doubling this parameter did not change the computed kinetic function significantly. χ should be regarded strictly as a noise control parameter and not a physical property of the fragmenting macromolecules. For further elaboration on the choice of χ see "Discussion" section.

Kinetic function exhibiting a maximum at intermediate molecular weight

In the previous example, the kinetic function increases with M_r reflecting the reduced stability of larger macromolecules. However, physical factors such as lower random Brownian motion of larger molecules may cause stability to increase beyond certain critical molecular weight. Under these conditions, the kinetic function may exhibit a maximum at some intermediate M_r. This behavior is exhibited by the following kinetic function[18]

$$K = (M_r, M_p) = 997.523 e^{-3M_r} M_p (M_r - M_p), \quad M_p \leq M_r \quad (18)$$

As shown in Figure 4a. This is a generalization of the kinetic function in Eq. 17 with the introduction of the explicit negative exponential dependence on M_r and the choice of two adjustable numerical parameters.

Following the presentation sequence of the previous example, the simulated MWD curves based on Eq. 18 are shown in Figure 4b. These are for the same set of measurement time steps shown in Figure 1b. The temporal behavior of $C(\tau, M)$ for a slightly different set of 11-point $\mathbf{M}_{seltm}$ are shown in Figures 5a, b. The temporal derivatives $\partial C(\tau, M)/\partial\tau$ obtained by numerical differentiation are shown in Figure 5c. The discrete points are the temporal derivatives stored as the column vector $\mathbf{\Phi}$. They are for the combinations of $\boldsymbol{\tau}_{selt}$ and the new $\mathbf{M}_{selm}$ as in the previous example,

The kinetic function extracted by Eq. 16 from the data in Figure 4b, is shown as discrete points in Figure 6. It is clear that this solution, with the exception of the discrete points for $M_r = 1$, is in very satisfactory agreement with the continuous curves from Figure 4a. See discussion below. To

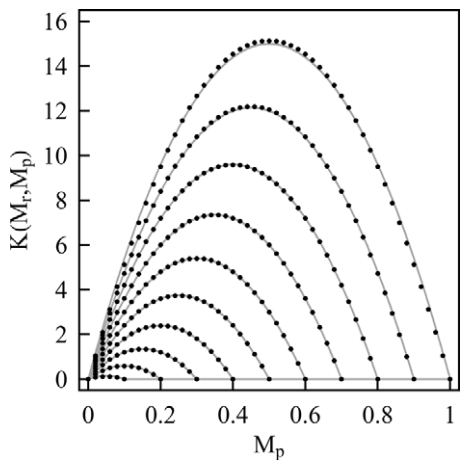

Figure 3. Comparison of kinetic functions.

Discrete points are the solution given by Eq. 16 and the light continuous curves are from Figure 1a.

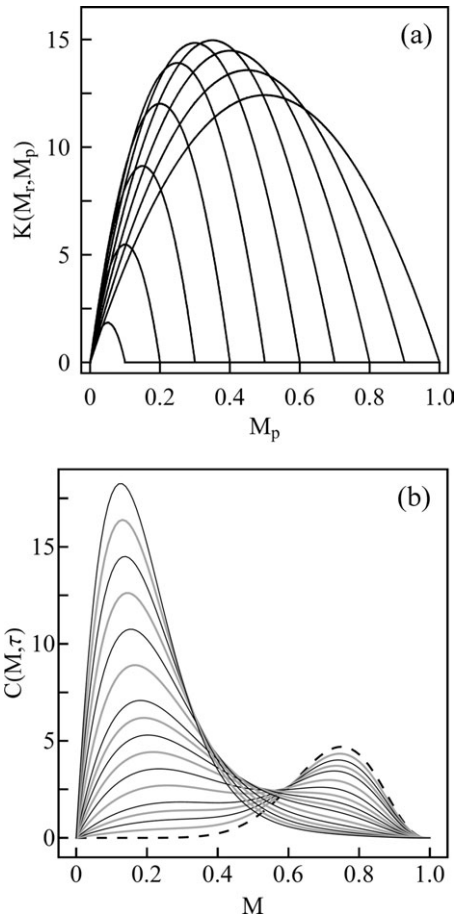

Figure 4. Kinetic function with intermediate maximum and MWD curves.

(a) Variation of kinetic function $K(M_r, M_p)$ from Eq. 18 with M_p. M_r is kept fixed at the same set of values as Figure 1a on each curve. (b) Simulated MWD curves $C(\tau, M)$ based on the kinetics in (a) for the same set of measurement time steps as in Figure 1b.

achieve this level of agreement the number of discretization points in molecular weight was increased to $N_D = 101$ to cope with the more rapid variation exhibited by the MWD curves. The corresponding $\chi = 0.0001$. The MoL solution of the direct problem using the computed kinetic function is, as in the previous example, essentially indistinguishable from the solution of the direct problem in Figure 4b.

Kinetic function with nonlinear dependence on molecular weights

In the investigation of particulate processes it is common practice to assume that the kinetics of particle fragmentation depends on the size of the participating particles raised to some semiempirical exponents.[19] In depolymerization kinetics this would correspond to raising the factors M_r, M_p and $(M_r - M_p)$ in the kinetic function $K(M_r, M_p)$ to some exponents. An arbitrary generalization of Eq. 18 along this line of reasoning is

$$K(M_r, M_p) = 31.991 \times 10^3 e^{-5M_r} M_p^2 (M_r - M_p)^2, \quad M_p \le M_r \tag{19}$$

This function is shown graphically in Figure 7a. It is used to test the performance of Eq. 16 in coping with more general kinetics. A set of simulated MWD curves based on this kinetics is shown in Figure 7b. These are for the same set of measurement time steps as in the previous examples.

The discrete points in Figures 8a, b show the temporal behavior of $C(\tau, M_r)$ for a set of $\mathbf{M}_{selm}$. To cope with anticipated numerical difficulties $\mathbf{M}_{selm}$ now has 13 points with additional points added for M close to 0 and 1. See figure

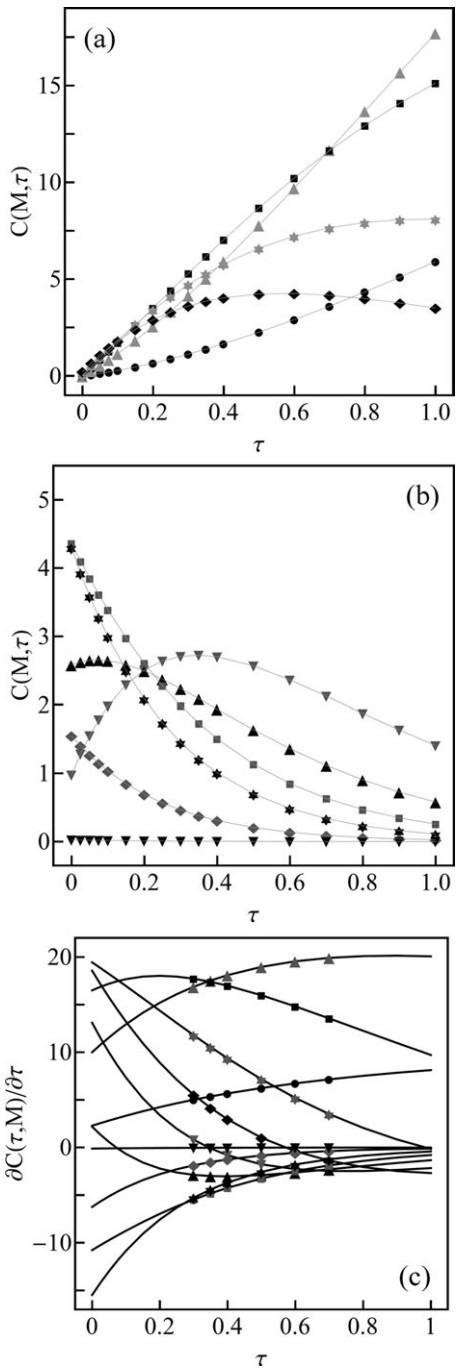

Figure 5. Temporal variation and temporal derivatives of $C(\tau, M)$.

(a) and (b) Plots of $C(\tau, M)$ based on Eq. 18 against τ. On each curve M is kept fixed at the indicated molecular weight $\mathbf{M}_{selm}$ = [0.02(●), 0.1(▲), 0.2(■), 0.3(★), 0.4(◆), 0.5(▼), 0.6(▲), 0.7(■), 0.8(★), 0.9(◆), 0.98(▼)]^T. (c) Variation of temporal derivatives with τ for the set of $\mathbf{M}_{selm}$ in (a) and (b). Discrete points are the derivatives at the same set of τ_{selt} in Figure 2c.

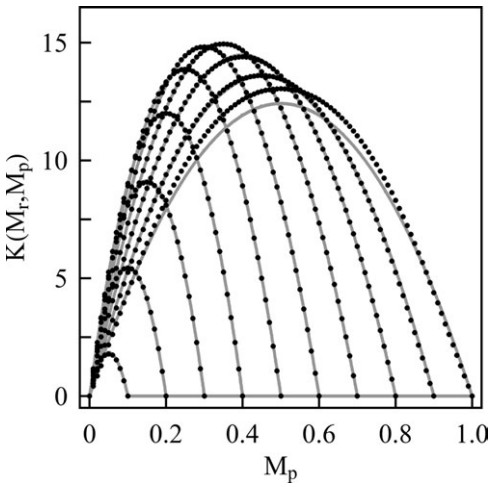

Figure 6. Comparison of kinetic functions.

Discrete points are the solution given by Eq. 16 and the light continuous curves are from Figure 4a.

caption. As before the temporal derivatives $\partial C(\tau, M_r)/\partial\tau$ generated by the first inverse problem are shown in Figure 8c. The discrete points are again the derivatives for the combinations of $\boldsymbol{\tau}_{selm}$ and $\mathbf{M}_{selm}$ stored as $\boldsymbol{\Phi}$ which now has $6 \times 13 = 78$ elements.

Following the presentation as the previous examples, the computed kinetic function given by Eq. 16 with $N_D = 101$ is displayed as discrete points in Figure 9. $\chi = 0.001$ for this set of results. For comparison the original kinetic function is shown as lighter curves on the same figure. The agreement

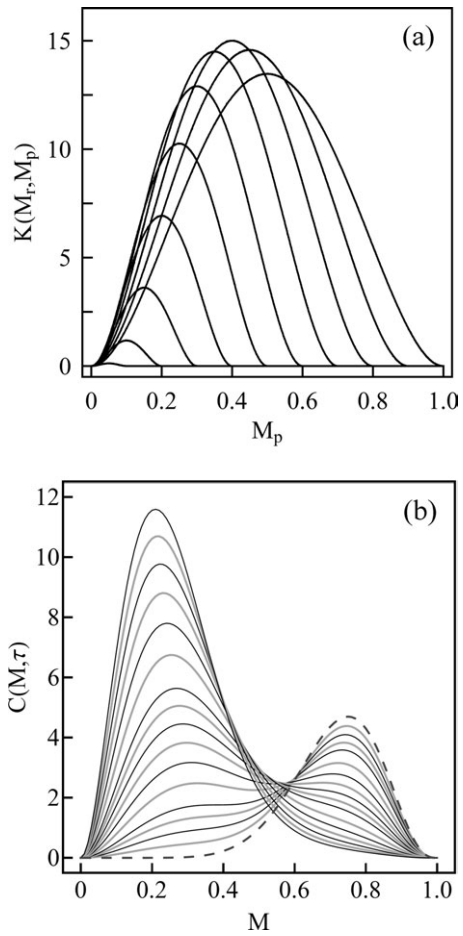

Figure 7. Nonlinear kinetic function and MWD curves.

(a) Variation of kinetic function $K(M_r, M_p)$ from Eq. 19 with M_p. M_r is kept fixed at the same set of values as Figure 1a on each curve. (b) Simulated MWD curves $C(\tau, M)$ based the kinetics in (a) for the same set of measurement time steps as in Figure 1b.

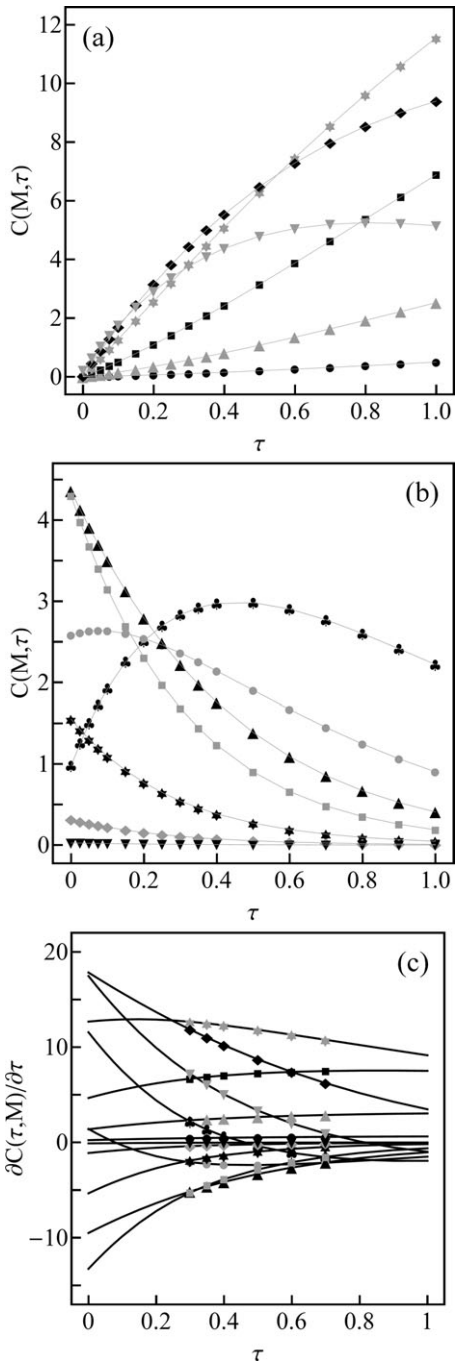

Figure 8. Temporal variation and temporal derivatives of $C(\tau, M)$.

(a) and (b) Plots of $C(\tau, M)$ based on Eq. 19 against τ. On each curve M is kept fixed at the indicated molecular weight M_{selm} = [0.02(●), 0.05(▲), 0.1(■), 0.2(★), 0.3(◆), 0.4(▼), 0.5(♣), 0.6(●), 0.7(▲), 0.8(■), 0.9(★), 0.95(◆), 0.98(▼)]^T. (c) Variation of temporal derivatives with τ for the M_{selm} in (a) and (b). Discrete points are the derivatives at the same set of τ_{selt} in Figure 2c.

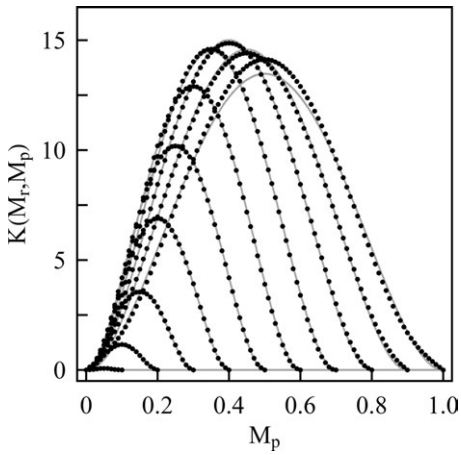

Figure 9. Comparison of kinetic functions.

Discrete points are the solution given by Eq. 16 and the light continuous curves are from Figure 7a.

between the discrete points and the continuous curves is very satisfactory with observable difference showing up only for $M_r > 0.95$. Again when the computed kinetic functions is used in the MoL solution of the direct problem of depolymerization the resulting MWD curves are essentially indistinguishable from that in Figure 7b.

Discussion

Obtaining the kinetic function speedily and reliably from a set of observed MWD data is a computational problem of immense practical interest. The examples show that the data manipulation and numerical steps described above have succeeded in solving this problem by treating it as two consecutive inverse problems. This success is attributed to the effectiveness of Tikhonov regularization in keeping noise amplification in check in both problems. In the first inverse problem discrete concentration density vs. time data are differentiated numerically to yield a smooth temporal derivative. The effectiveness of Tikhonov regularization in keeping noise under control in numerical differentiation is well documented in the literature. The second inverse problem can be regarded as one of solving a set of linear algebraic equations for the discretized kinetic function. In this problem the number of unknowns exceeds the number of equations. Tikhonov regularization is known to be effective in ensuring that the resulting solution does not exhibit physically unrealistic fluctuations. This too is well documented - certainly for one-dimension problem and to a slightly lesser extent for its higher-dimension counterparts. It is therefore reasonable to expect the two-step procedure centered around Tikhonov regularization to perform well in solving the inverse problem of depolymerization.

While it is true that all the results reported above are based on simulated MWD data it should be emphasized that the solution procedure treats these data as discrete numerical input completely independent of their origin and functional form. The procedure also made no reference at all to the kinetic functions used to generate the simulated data or any assumption regarding their functional forms. This is very different from the popular procedure in the literature for investigating the kinetics of depolymerization in which an educated guess of the functional form of $K(M_r, M_p)$ has to be made followed by an iterative procedure to determine the parameters in the assumed functional form. As already mentioned such a process often does not result in an acceptable kinetic function. In direct contrast the present procedure of determining $K(M_r, M_p)$ does not involve lengthy iterative computation. It only requires the relatively simple matrix operations in Eq. 16. All the matrices associated with this equation are just as simple to set up.

To ensure that the temporal derivatives $\partial C(\tau, M_r)/\partial\tau$ derived from the discrete data in Figures 2, 5, and 8 are reliable it is essential that, for each selected M_{selm}, the number of data points on the evolving $C(\tau, M_{selm})$ curve is large enough for Tikhonov regularization to work properly. Experience shows that, depending on the noise level in the data, typically the data need to have 15 to 20 points. It was also observed that the derivative associated with discretization points close to the two ends of the data set are less reliable.[15] For this reason only $\partial C(\tau, M_r)/\partial\tau$ derived from internal discretization points of the data set were selected as the RHS of the second inverse problem. Most of the depolymerization MWD data in the literature only include between 3 and 10 measurement time steps. This makes the resulting $\partial C(\tau, M_r)/\partial\tau$, for any M_{selm}, unreliable. This has prevented the application of the present procedure to existing experimental MWD curves. However, as MWD measurement by GPC is further developed and automated, data sets with sufficient number of time steps for $\partial C(\tau, M_r)/\partial\tau$ evaluation will become the norm.

In all the results presented above the size of the selected dimensionless time τ_{selt} was kept fixed at $\Omega = 6$. Numerical experimentation revealed that, with the quality of the temporal derivatives $\partial C(\tau, M_r)/\partial\tau$ in Figures 2c, 5c, and 8c, Ω can be reduced to as small as 3 to 4 points without significant deterioration in the resulting kinetic function $K(M_r, M_p)$. This observation is clearly dependent on the quality of the temporal derivatives generated by numerical differentiation in the first inverse problem. This quality depends greatly on the error bars associated with these data as well as the number of measurement time steps. It is reasonable to expect that the detrimental effects of random errors in the temporal derivatives can be ameliorated by enlarging the size of τ_{selt}.

The temporal derivative $\partial C(\tau, M_{selm})/\partial\tau$ on the RHS of Eq. 6 is generally positive for large M_{selm} and negative for small M_{selm}. In setting up the second inverse problem it is sensible to aim for even coverage of this spread in values. This is achieved by making, as mentioned above, $\mathbf{M}_{selm}$ every tenth element of the discretized molecular weight $\mathbf{M}$. There is actually a considerable degree of freedom in assembling the set $\mathbf{M}_{selm}$ both in terms of number and distribution of elements in the set. The only restriction is that, for programming simplicity, $\mathbf{M}_{selm}$ has to be a subset of $\mathbf{M}$. To reduce the size of the computation problem some elements of $\mathbf{M}_{selm}$ can be left out. For example, examination of Figures 2c, 5c, and 8c shows that for some M_{selm} the $\partial C(\tau, M_{selm})/\partial\tau$ is close to zero. It was observed that some of the Eq. 6 with RHS close to zero can be selectively thinned out without detrimental effects. Conversely if there are molecular weights where the derivatives $\partial C(\tau, M_{selm})/\partial\tau$ exhibit significant features these clearly should be included in $\mathbf{M}_{selm}$. The setup of the computation scheme has the flexibility to cope with such special cases.

$K(M_r, M_p)$ is a function of two independent variables therefore the second inverse problem requires regularization in two dimensions. The decision, in the present investigation, to minimize the SoQ of $\partial^2 K/\partial M_r^2$ and that of $\partial^2 K/\partial M_p^2$ in

the Tikhonov regularization computation is at odd with the usual recommendation of minimizing the SoQ of the Laplacian ($\partial^2 K/\partial M_r^2 + \partial^2 K/\partial M_p^2$) for two-dimension regularization.[12,16] This is best regarded as a numerical expediency. With central difference approximation, the Laplacian can only be evaluated at internal discretization points without introducing additional unknowns. Minimizing the SoQ of Laplacian restricted to the internal discretization points resulted in unacceptable fluctuations in the resulting $K(M_r, M_p)$ for $M_r = 1$. While the second derivative $\partial^2 K/\partial M_r^2$ at $M_r = 1$ cannot be approximated by central difference without special modification, this can be done with the second derivative $\partial^2 K/\partial M_p^2$. It can therefore be included in the SoQ minimization of second derivatives. This has the effect of suppressing the undesirable/unphysical fluctuation observed in regularization based on the Laplacian. Such an ad hoc modification of the regularization procedure clearly requires further analysis and justification. Other modifications, such as using different finite difference schemes to approximate the second partial derivatives of $K(M_r, M_p)$ should also be explored. All these are beyond the scope of the present investigation.

The results in Figures 3, 6, and 9 show the common trend of increasing error in the computed kinetic function in the neighborhood of $M_r = 1$. A quick examination of the numerical coefficients associated with $K(M_r = 1, M_p)$ in Eq. 6 will reveal the basic cause of this trend. These coefficients are identically zero as $C(\tau, M_r) = 0$ for $M_r = 1$ and close to zero for M_r close to unity. This implies that the value of kinetic function in this neighborhood is not determined by the governing equation of depolymerization but is instead a consequence of regularization.

As already mentioned the **K** matrix is very large even for moderate N_D. But after the reduction based on Eq. 7 the actual number of unknowns in the Eq. 16 becomes quite manageable. The resulting problem can easily be handled by computers with 4G RAM. Computation with $N_D = 101$ takes no more than 3 to 4 mins on a typical 2GHz machine. This is assuming that all the temporal derivatives $\partial C(\tau, M_r)/\partial\tau$ from the first inverse problem have been computed beforehand and stored as a column vector **Φ** ready to be retrieved when required.

With increasing depolymerization time large numbers of smaller-sized macromolecules are likely to be produced. These show up in the evolving MWD curves as narrow peaks at low molecular weight m. This raises the issue of numerical resolution needed to deal with these peaks. In principle by increasing N_D it is possible for the discretization scheme, uniform in m, to capture these peaks. This is an ineffective way of coping with the numerical resolution issue. With $N_D > 301$ or thereabout the two-step regularization scheme is likely to require RAM in excess of 4 GB. More significantly the main bulk of the additional discretization points are located at large m where increase in resolution in not required. Recently, in their treatment of the direct problem of flocculation, Yeow et al. demonstrated that this resolution issue can be overcome by adopting $\log_{10} m$, instead of m, as the independent variable and introducing a discretization scheme that is uniform in the logarithmic variable.[20] This development can be adapted for the solution of the inverse problem of depolymerization where the MWD curves exhibit narrow peaks. Adoption of $\log_{10} m$ as the independent variable in the inverse problem of depolymerization (and of flocculation) requires complete reformulation of the governing equations and the corresponding details of the numerical solution procedure. This is currently being investigated.

In any application of Tikhonov regularization the choice of the regularization parameter χ is always an issue. For the one-dimension regularization of the first inverse problem the guidelines for setting χ is well researched and reported. These include the method of GCV,[21] the L-curve[22] and the Morozov principle.[11] For the two-dimension regularization of the second inverse problem, a search of the literature has failed to locate an easy to implement method for selecting χ. Instead, as previously mentioned, for the second inverse problem the adjustment of χ was based on a simple and physically obvious reasoning. It was adjusted so that the difference between the LHS and RHS of Eq. 9 is kept small, typically within about 10%, and which at the same time resulted in a $K(M_r, M_p)$ that is relatively free of unreal fluctuations. This can usually be achieved with a few trial values of χ in Eq. 16. A final test can always be performed by using the $K(M_r, M_p)$ given by Eq. 16 in the MoL solution of the direct problem of depolymerization and compare this outcome against the original MWD curves. This test revealed that only the order of magnitude of χ is important and there is no necessity to preform fine adjustment of this parameter. Until a simple easy to implement guide based on statistical or error analysis is available for higher-dimension regularization the practical approach adopted here will probably suffice for most practical situations.

Conclusion

The PBE of depolymerization when reformulated as an inverse problem provides a direct path for converting observed MWD data to kinetic function. The numerical procedure, based on two consecutive applications of Tikhonov regularization, is a reliable way of solving this inverse problem. The procedure is general in that it is not restricted to MWD data or kinetic function of specified forms. The constituent steps of the procedure are conceptually easy to understand and computationally simple to implement. Unlike currently popular methods for obtaining kinetic function, the procedure does not involve extensive iterative computation and can be performed using general purpose scientific computing software running on present day laptops.

Notation

$\mathbf{A}$ = composite matrix $\boldsymbol{\alpha}$ and $\boldsymbol{\beta}$ Eq. 13
c = concentration density function mole m^{-3} (mol wt)$^{-1}$
C = dimensionless concentration density function = $(m_{max})^2 \times c/m_{total}$ Eq. 5
$\mathbf{D}$ = composite column vector **E** and **F** Eq. 12
$\mathbf{E}, \mathbf{F}$ = column vector of second derivatives of Γ Eq. 13
$\mathbf{G}$ = $\Omega \times \Lambda$ matrix of coefficients from LHS of discretized Eq. 8
$\mathbf{H}$ = matrix of $\partial C/\partial\tau$ at selected time and molecular weight
$H_{selt,selm}$ = elements of **H**
k = fragmentation kinetic function, (mol wt)$^{-1} \times s^{-1}$ Eq. 3
K = dimensionless fragmentation kinetic function = $k \times t_{max} \times m_{max}$ Eq. 5
$\mathbf{K}$ = matrix of discretized K
$K_{i,j}$ = elements of **K**
m = molecular weight
m_p = molecular weight of fragmentation product
m_r = molecular weight of fragmenting molecule
m_{total} = total mass of macromolecules, kg m^{-3}

$\mathbf{m}_{\text{selm}}$ = selected set of molecular weight
M = dimensionless molecular weight = $m/m_{\max}$
N_{D} = number of discretization points
R = residual Eq. 15
t = fragmentation time, s

Greek letters

$\boldsymbol{\alpha}$, $\boldsymbol{\beta}$ = matrices of numerical coefficients arising from central difference Eq. 12
$\alpha_{\zeta,\lambda}$, $\beta_{\zeta,\lambda}$ = elements of matrices $\boldsymbol{\alpha}$, $\boldsymbol{\beta}$
$\boldsymbol{\Gamma}$ = column vector of independent unknown $K_{i,j}$
Γ_{λ} = element of column vector $\boldsymbol{\Gamma}$
Δ = discretization step size = $(1\text{-}M_{\min})/(N_{\text{D}}\text{-}1)$
Λ = total number of unknown Γ_{λ}
$\mu_{i,\text{selm}}$, $v_{\text{selm},j}$ = coefficients of trapezoidal rule quadrature Eq. 8.
Σ = total number of selected molecular weight
τ = dimensionless time = $t/t_{\max}$ Eq. 5
$\boldsymbol{\tau}_{\text{selt}}$ = a set of selected τ
$\boldsymbol{\Phi}$ = elements $\mathbf{H}$ rearranged as column vector
Φ_{ω} = element column vector $\boldsymbol{\Phi}$
χ = Tikhonov regularization parameter Eq. 15
Ψ = total number of Φ_{ω}
Ω = total number of $\Phi_{\omega} = \Psi \times \Sigma$

Subscripts

i, j = positive integers, general indices
max = maximum
min = minimum
selm = positive integer, index of $\mathbf{m}_{\text{selm}}$
selt = positive integer, index of $\boldsymbol{\tau}_{\text{selm}}$
ζ = positive integer, general indices
λ, ω = positive integers indices of column vectors $\boldsymbol{\Gamma}$ and $\boldsymbol{\Phi}$, respectively

Literature Cited

1. Aris R. On reactions in continuous mixtures. *AIChE J*. 1989;35: 539–548.
2. Wu C-S, editor. *Handbook of Size Exclusion Chromatography and Related Techniques*, 2nd ed. New York: Marcel Dekker, 2004.
3. Wang M, Zhang C, Smith JM, McCoy BJ. Continuous-mixture kinetics of thermolytic extraction of coal in supercritical fluid. *AIChE J*. 1994;40:131–142.
4. Robertson JE. Thermal degradation studies of polycarbonate. PhD thesis. Virginia Polytechnic Institute and State University, 2001.
5. Mahammad S, Prud'homme RK, Roberts GW, Khan SA. Kinetics of enzymatic depolymerization of guar galactomannan. *Biomacromolecules*. 2006;7:2583–2590.
6. Randolph AD, Larson MA. *Theory of Particulate Processes*, 2nd ed. San Diego: Academic Press, 1988.
7. Ramkrishna D. *Population Balances. Regularization of Inverse Problems*. San Diego: Academic Press, 2000.
8. Schiesser WE. *The Numerical Method of Lines*. San Diego: Academic Press, 1991.
9. Yeow YL, Guan B, Wu L, Yap T-M, Leong Y-K. Obtaining the evolving concentration distribution curves during binary disintegration of macromolecules. *AIChE J*. 2008;54:2699–2706.
10. Sathyagal A, Ramkrishna D, Narsimhan G. Solution of inverse problems in population balances. II. Particle break-up. *Comput Chem Eng*. 1995;19:437–451.
11. Engl HW, Hanke M, Neubauer A. *Regularization of Inverse Problems*. Dordrecht: Kluwer Academic, 2000.
12. Aster RC, Thurber CH, Borchers B. *Parameter Estimation and Inverse Problems*. Amsterdam: Elsevier Science, 2005.
13. Ziff RM, McGrady ED. Kinetics of polymer degradation. *Macromolecules*. 1986;19:2513–2519.
14. Brunner H. *Numerical solution of initial-value problems for integro-differential equations*. In: Griffiths DF, Watson GA, editors. *Numerical Analysis 1987, Pitman Research Notes in Mathematics*, Vol. 170. London: Longmans, 1989:18–38.
15. Lubansky AS, Yeow YL, Leong Y-K, Wickramasinghe SR, Han B. A general method of computing the derivative of experimental data. *AIChE J*. 2006;52:323–332.
16. Press WH, Teukolsky SA, Vetterling WT, Flannery BP. *Numerical Recipes*, 4th ed. Cambridge: Cambridge University Press, 2007.
17. McCoy BJ, Wang M. Continuous-mixture fragmentation kinetics: particle size reduction and molecular cracking. *Chem Eng Sci*. 1994;49:3773–3785.
18. McCoy BJ, Madras G. Evolution to similarity solutions for fragmentation and aggregation. *J Colloid Interface Sci*. 1998;201:200–209.
19. Han B, Akeprathumchai S, Wickramasinghe SR, Qian X. Flocculation of biological cells: experiment vs. theory. *AIChE J*. 2003;49:1687–1701.
20. Yeow YL, Liow J-L, Leong Y-K. A general procedure for obtaining the evolving particle size distribution of flocculating suspensions. *AIChE J*. In press.
21. Wahba G. *Spline Models for Observational Data*. Philadelphia, PA: SIAM, 1990.
22. Hansen PC. Analysis of discrete ill-posed problems by means of the L-curve. *SIAM Rev*. 1992;34:561–580.

Manuscript received Mar. 7, 2012, and revision received June 2, 2012.